Effect of collisions on line profiles in the vibrational spectrum of molecular hydrogen

J. D. Kelley and S. L. Bragg
McDonnell Douglas Research Laboratories, St. Louis, Missouri 63166
(Received 25 April 1986)

A semiclassical calculation of density-broadening and line-shift coefficients in the vibrational-rotational spectrum of molecular hydrogen is presented. These parameters are obtained as functions of temperature and upper-state quantum numbers, and the calculated results are in good agreement with experimental values obtained from fundamental and overtone electric quadrupole spectra, except for the 4-0 overtone density-broadening coefficient. Results from Raman and electric-field-induced spectra in the fundamental band are also discussed. The calculation includes construction of an intermolecular potential for the H_2-H_2 interaction. The vibrational phase shift resulting from collision is shown to account for the vibrational state dependence of the broadening and shift coefficients, and the observed temperature dependence of the line shift is reproduced by the calculation.

I. INTRODUCTION

The vibrational-rotational spectrum of gas-phase molecular hydrogen is of interest for several reasons. Astronomers observe the electric quadrupole spectrum of hydrogen in the major planets and use these observations to model the planetary atmospheres.[1] Accurate quantum-mechanical calculations of the H-H interaction potential[2] are available, and these calculations allow critical comparisons of calculated and observed line positions. Similarly, experimentally observed quadrupole-absorption line strengths can be compared with theoretical values.

Line shifts and broadening in H_2 resulting from collisions with H_2 or a foreign gas are of considerable theoretical interest. These parameters probe the intermolecular interaction potential, and they can provide information on both the angular and radial dependence of the interaction. A sequence of overtone transition measurements provides additional valuable data on the dependence of the interaction potential on the H_2 vibrational coordinate.

For all these reasons, there have been numerous experimental studies of the molecular hydrogen spectrum. The first observation of a vibrational transition in hydrogen was made in the electric quadrupole spectrum by Herzberg.[3] There have been several subsequent quadrupole-absorption measurements.[4–9] Line-shift coefficients have been measured for the fundamental absorption band,[4,8,9] the first overtone,[5,8,9] and higher overtones.[6–9] Broadening coefficients for the fundamental[4,9] and various overtone transitions[9] have also been determined. In addition to the quadrupole-absorption studies, the fundamental band of H_2 has been observed in the electric-field-induced spectrum[10–12] and in the Raman spectrum.[13–19] Line-shape parameter values are provided by these studies. A comparison of the density broadening and shift coefficients obtained in the various measurements forms part of the discussion below.

This publication summarizes the extensive set of H_2 quadrupole-absorption measurements previously obtained by one of us;[9] included in this summary are results which have not previously appeared in publication. A theoretical calculation of collision-induced line shifts and self-broadening coefficients in the 1-0 through 4-0 vibrational bands is also presented. The calculation uses some simplifying characteristics of hydrogen and its isotopes to obtain the vibrational dependence of the shift and broadening coefficients.

II. OUTLINE OF CALCULATIONS

The semiclassical line-shape theory of Anderson[20] has formed the basis for many subsequent theoretical studies of the effects of molecular collisions on the shape of spectral lines, and the approach here is a modified version of the Anderson approach.

In the Anderson theory[20,21] the linewidth [half width at half maximum (HWHM)] is given by

$$\Delta\omega_{1/2}=n\bar{u}\sigma_r \tag{1}$$

and the line shift by

$$\omega-\omega_0=n\bar{u}\sigma_i\ . \tag{2}$$

In these equations, n is the perturber number density, u is the relative collision velocity, and $\bar{u}=\int_0^\infty uf(u)du$ denotes an equilibrium average. The quantities σ_r and σ_i are the real and imaginary parts of the optical cross section σ. For isolated lines and collision times short compared with the time between collisions,[22]

$$\bar{u}\sigma(v_ij_iv_fj_f)=\int_0^\infty uf(u)du\int_0^\infty F(u,b)2\pi b\,db\ . \tag{3}$$

with

$$F(u,b)=\sum_{m_f,m_{f'},m_i,m_{i'},m_k}(-1)^{m_f-m_{f'}}\begin{pmatrix}j_i & k & j_f\\ m_i & -m_k & -m_f\end{pmatrix}\begin{pmatrix}j_i & k & j_f\\ m_{i'} & -m_k & -m_{f'}\end{pmatrix}$$
$$\times[\delta(m_im_{i'})\delta(m_fm_{f'})-\langle v_fj_fm_{f'}\,|\,S^*(u,b)\,|\,v_fj_fm_f\rangle\langle v_ij_im_{i'}\,|\,S(u,b)\,|\,v_ij_im_i\rangle]\ . \tag{4}$$

In Eqs. (3) and (4), b is the impact parameter of the collision, $v_i j_i$ and $v_f j_f$ label the vibrational-rotational states connected by the optical transition, and k is the tensor order of the transition ($k=0$ for an isotropic Raman transition, 1 for a dipole transition, and 2 for an electric quadrupole or anisotropic Raman transition). The m's are projection quantum numbers. The quantity $S(u,b)$ is the S matrix associated with a radiator-perturber collision of velocity u and impact parameter b; in using Eq. (4) we assume that the radiator and perturber molecules can be distinguished. This assumption is satisfactory even for self-broadening or shifting except when the possibility of resonance effects exists. The formal correction for such effects and the practical implications for self-broadening and shifting in H_2 will be discussed in Sec. V below.

The differences among various semiclassical approaches to the calculation of collisional effects on line shapes arise from the different approaches employed in the calculations of $S(u,b)$. In Anderson's original treatment, the relative motion in the collision coordinates was considered a set of straight-line trajectories for all u and b, and the S matrix was approximated as an expansion to second order in the interaction potential. The work of Fiutak and Van Kranendonk[23,24] on self-broadening in hydrogen is a relevant example of this type of treatment.

The straight-line-trajectory assumption causes problems in the second-order expansion, because the S-matrix elements depend on the time-integrated interaction potential, and for interactions of the form $V_I=CR^{-n}$, the integral $\int_{-\infty}^{+\infty} V_I[R(t)]dt$ diverges for $b\to 0$, or $R(t)\to ut$. To avoid this difficulty a lower limit for b is introduced.[21]

A more realistic treatment of the classical collision trajectory is to solve the equations of motion using the spherically symmetric part of the interaction potential. This avoids the divergence for $b\to 0$ and the calculation can be done for all b. It is still possible in some cases that the interaction strength is sufficiently large that a second-order expansion is not adequate, and a unitary treatment of the S matrix which includes inelastic collision processes if necessary, is required. Examples of such treatments can be found in the work of Nielsen and Gordon[22] and Smith, Giraud, and Cooper.[25]

Theoretical treatment of collision broadening and the shift in line center for the vibrational-rotational lines of molecular hydrogen is simplified somewhat by the fact that σ_r and σ_i are both small ($\approx 10^{-2}$ times gas kinetic cross section). This allows separation of the phase shift, reorientation (m changing), and inelastic (j or v changing) collisional contributions to these cross sections. This separation is seen most easily by using Gordon's[26] classical-limit expressions for σ_r and σ_i. For S-branch electric quadrupole transitions Gordon[26] obtains

$$\sigma_r=\bar{u}^{-1}\int_0^\infty uf(u)du\int_0^\infty [1-\cos(\eta)P_{el}\cos^4(\alpha/2)]2\pi bdb\ , \tag{5}$$

$$\sigma_i=\bar{u}^{-1}\int_0^\infty uf(u)du\int_0^\infty \sin(\eta)P_{el}\cos^4(\alpha/2)2\pi bdb\ , \tag{6}$$

where η is the total phase shift, α is the reorientation angle and P_{el} is the probability that no changes in j or v occur in the collision characterized by u and b. Similar expressions can be obtained for the Q and O branches.

If Eq. (5) is rewritten with $\cos\eta=1-g(\eta)$, then

$$\sigma_r=\bar{u}^{-1}\int_0^\infty uf(u)du\int_0^\infty \{[1-P_{el}\cos^4(\alpha/2)]+g(\eta)P_{el}\cos^4(\alpha/2)\}2\pi bdb\ . \tag{7}$$

The term in square brackets is the contribution to σ_r due to rotational inelasticity and/or reorientation in the absence of any phase shift; when averaged over b and u this term will be comparable with the broadening cross section for a transition in the rotational spectrum. Because the experimentally determined rotational broadening cross sections are small, about 0.4×10^{-16} cm^2 for H_2, and because they can be adequately reproduced by a second-order Anderson-type treatment,[27,28] it is safe to assume that $P_{el}\cos^4(\alpha/2)\simeq 1$ for most of the u,b range.

Equations (1) and (2) can now be rewritten, using Eqs. (7) and (6), as

$$\Delta\omega_{1/2}=n(\gamma_R+\gamma_v)\ , \tag{8}$$

$$\omega-\omega_0=n\delta_v\ . \tag{9}$$

In these expressions γ_R and γ_v represent rotational and vibrational contributions to the density-broadening coefficient γ, and δ_v represents the vibrational contribution to the line-center-shift coefficient. The subscript notation anticipates the results presented below; the Δj and Δm contributions are purely rotational in origin, and by far the largest contribution to the phase shift is vibrational in origin so that $\delta_R\simeq 0$ and $\delta\approx\delta_v$. Moreover, the phase shift is the only contribution the vibrational degree of freedom makes to the self-broadened H_2 line shape; the vibrational spacing and anharmonicity are large enough that vibrationally inelastic processes (vibration-translation and vibration-vibration energy transfer) make a negligible contribution.

The foregoing considerations allow considerable simplification in the calculation of density broadening and shift coefficients for fundamental and overtone transitions in H_2. The separability of γ_R and γ_v for H_2 allows these contributions to be obtained independently. Experimental values for γ_R obtained from the pure rotational spectrum can be used in conjunction with calculated γ_v's for the fundamental and overtone vibrational transitions to obtain total-broadening coefficients γ, and the line-shift coefficients δ can be equated to δ_v to a good approximation. The calculation is then reduced to obtaining the collisional phase shifts $\eta(b,u)$ associated with the vibrational motion, and then integrating $\cos\eta$ and $\sin\eta$ over b and u to obtain

$$\gamma_v=\int_0^\infty uf(u)du\int_0^\infty (1-\cos\eta)2\pi bdb\ , \tag{10}$$

$$\delta_v=\int_0^\infty uf(u)du\int_0^\infty \sin(\eta)2\pi bdb\ . \tag{11}$$

In the semiclassical formulation used here,

$$\eta_{i,f}(b,u)=\langle\Psi_f(\mathbf{r}_1,\mathbf{r}_2)|\int_{-\infty}^{+\infty}V_I(\mathbf{r}_1,\mathbf{r}_2,t)dt\,|\Psi_f(\mathbf{r}_1,\mathbf{r}_2)\rangle-\langle\Psi_i(\mathbf{r}_1,\mathbf{r}_2)|\int_{-\infty}^{+\infty}V_I(\mathbf{r}_1,\mathbf{r}_2,t)dt\,|\Psi_i(\mathbf{r}_1,\mathbf{r}_2)\rangle\ , \tag{12}$$

where i and f are the initial and final states of the two-molecule collision system and $V_I(\mathbf{r}_1,\mathbf{r}_2,t)$ is the time-dependent interaction potential with the relative H_2-H_2 motion described by a classical trajectory defined by b and u.

The total calculated density-broadening coefficient γ for an S-branch transition $(0,j\rightarrow v,j+2)$ can be constructed by adding the experimental value for γ_R obtained from the pure rotational spectrum $(0,j\rightarrow 0,j+2)$ to the calculated γ_v as indicated in Eq. (8). The data of Keijser *et al.*[27] were used here to obtain γ_R, as shown in Table I.

Obtaining γ for the Q branch is less direct because there is no rotational Q branch, so that γ_R is not directly available. The contribution of γ_R to the total Q-branch γ values can be estimated by subtracting the calculated γ_v from the total γ values observed in the Q-branch fundamental spectrum. These estimated γ_R values can then be used for calculating γ in the overtone transitions. This approach to obtaining the S- and Q-branch γ values relies on the separability of rotational and vibrational contributions to the total broadening and the expectation that γ_R is essentially independent of vibrational quantum number.

TABLE I. Rotational contribution γ_R to line-broadening coefficient. Values derived from results in Ref. 27 for the pure rotational spectrum.

Rotational transition	γ_R (10^{-3} cm^{-1}amagat^{-1} at 300 K)
$S(0)$	1.4
$S(1)$	1.7
$S(2)$	1.2
$S(3)$	1.2

III. INTERACTION POTENTIAL

An accurate intermolecular potential for the H_2-H_2 collision system is a prerequisite for calculation of the broadening and shift coefficients. An "exact" potential would allow calculation of any observable property determined by pairwise interactions in a molecular hydrogen system. For example, in addition to the line-shape parameters of interest here, elastic scattering cross sections should be accurately obtainable from the interaction potential. Thus, in a space-fixed coordinate system, the potential function must have the proper dependence on the intermolecular separation R and associated orientation angles Θ and Φ, the orientation angles for molecules 1 and 2, θ_1,ϕ_1 and θ_2,ϕ_2, and vibrational coordinates r_1 and r_2.

To our knowledge there is no highly accurate H_2-H_2 interaction potential available in the literature which satisfies all these criteria. However, there is an accurate "rigid-rotor" potential which does not include the r_1,r_2 dependence.[29] The complete interaction potential can be written in the form[30]

$$V_I(\mathbf{r}_1,\mathbf{r}_2,\mathbf{R})=V_{000}(r_1,r_2,R)+\sum_{l_1l_2\lambda}(4\pi)^{-3/2}V_{l_1l_2\lambda}(r_1,r_2,R)\sum_{m_1m_2m}Y_{l_1m_1}(\theta_1,\phi_1)Y_{l_2m_2}(\theta_2,\phi_2)Y^*_{\lambda m}(\Theta\Phi)\,, \tag{13}$$

where the Y's are spherical harmonics and $V_{l_1l_2\lambda}$ are themselves sums of terms that represent the short- and long-range contributions to V_I. The first term in the $l_1l_2\lambda$ sum is explicitly indicated as V_{000}.

The results of Norman, Watts, and Buck[29] (NWB) provide a rigid-rotor potential of the form indicated in Eq. (13) but with r_1 and r_2 replaced by r_0 ($r_0=0.767\times10^{-8}$ cm), the average H-H separation for H_2 in $v=0,j=0$. To incorporate the effect of bimolecular collision on H_2 vibrational motion, an explicit r_1,r_2 dependence must be added to the rigid-rotor interaction.

An estimate of the r_1,r_2 dependence in V_I can be made by inference from the accurate *ab initio* H_2-He interaction potential calculated by Meyer, Hariharan, and Kutzelnigg[31] (MHK) and refined by Senff and Burton.[32] The leading terms in the H_2-He potential, i.e., V_{000} and the equivalent pair V_{022} and V_{202}, each have a counterpart in the H_2-H_2 potential. The hydrogen system also has $V_{22\lambda}$ terms which do not appear for H_2-He; the quadrupole-quadrupole interaction is included in $V_{22\lambda}$. Given the similarity between He and H_2 as collision partners for H_2, one can use the working hypothesis that the fractional change with varying r_1 (or r_2) in each constituent term of V_{200}, V_{202}, or V_{022} for H_2-H_2 is the same as that for H_2-He.

Specifically, we begin with

$$V_{000}(r_1,r_2,R)=V_{\rm rep}(r_1,r_2,R)-f(R)\left[\frac{C_6(r_1,r_2)}{R^6}+\frac{C_8(r_1,r_2)}{R^8}+\frac{C_{10}(r_1,r_2)}{R^{10}}\right], \tag{14}$$

with similar expressions for V_{202} and V_{022}. The subscript rep refers to the repulsive potential terms. The function $f(R)$ serves to damp the contribution of the long-range terms for small R and has the form

$$f(R)=\begin{cases}\exp[-p(R^*/R-1)^2], & R\leq R^*\\ 1, & R\geq R^*\,.\end{cases} \tag{15}$$

The parameter p is unity for V_{000}, V_{022}, and V_{202}; R^* is 5.1×10^{-8} cm for V_{000} and 5.8×10^{-8} cm for V_{202} and V_{022}.

In the H_2-He interaction potential, the coefficients $C_n(r)$ arise almost entirely from the dispersion interaction[31] and therefore depend on the polarizabilities of the collision partners. Expanding the $C_n(r)$ for H_2-He in a Taylor series to second order about $r=r_0$, we obtain

$$C_n(r)=C_n(r_0)[1+\alpha_n(r-r_0)+\beta_n(r-r_0)^2], \tag{16}$$

where

$$\alpha_n = \frac{1}{C_n(r_0)} \frac{dC_n}{dr}\bigg|_{r_0} , \tag{17}$$

$$\beta_n = \frac{1}{2} \frac{1}{C_n(r_0)} \frac{d^2C_n}{dr^2}\bigg|_{r_0} . \tag{18}$$

A similar second-order expansion for H_2-H_2 yields

$$C_n(r_1,r_2) = C_n(r_0,r_0)\{1+\alpha_n[(r_1-r_0)+(r_2-r_0)]+\alpha_n^2(r_1-r_0)(r_2-r_0)+\beta_n[(r_1-r_0)^2+(r_2-r_0)^2]\} , \tag{19}$$

where the coefficients α_n and β_n for H_2-H_2 are partial derivatives with respect to r_1 or, equivalently, r_2 as in Eqs. (17) and (18). Insofar as the C_n values are solely functions of the polarizabilities of the collision pair, α_n and β_n are identical in Eqs. (16) and (19) because they are determined by the rate of change of the polarizability of H_2 with intramolecular separation. MHK give values of C_n for three r values, including r_0; these allow evaluation of α_n and β_n for the long-range terms in V_{000} and V_{202}, V_{022}. The values of $C_n(r_0)$, α_n, and β_n are shown in Table II.

A similar procedure can be used to estimate α_{rep} and β_{rep} in the expansions

$$V_{rep}(r_1,r_2,R) = V_{rep}(r_0,r_0,R)\{1+\alpha_{rep}[(r_1-r_0)+(r_2-r_0)]+\alpha_{rep}^2(r_1-r_0)(r_2-r_0)+\beta_{rep}[(r_1-r_0)^2+(r_2-r_0)^2]\} , \tag{20}$$

where

$$V_{rep}(r_0,r_0,R) = A\exp(-cR-dR^2) . \tag{21}$$

If the MHK results for H_2-He are used, one finds that α_{rep} and β_{rep} are not constants, but vary slowly with R. In addition, there is no reason to assume that the valence interactions responsible for the repulsive parts of V_{000} or V_{202}, V_{022} should be more than approximately the same in H_2-H_2 and H_2-He. Nonetheless, the H_2-He results can be used to provide initial values of α_{rep} and β_{rep}, and these can be refined using the experimental data as discussed below. The initial values were obtained by evaluating $\partial V_{rep}/\partial r$ and $\partial^2 V_{rep}/\partial r^2$ for H_2-He at $R = 2.64\times10^{-8}$ cm, near the turning point of $V_{000}(r_1,r_2,R)$ for a direct collision with average energy at $T = 300$ K. The initial values based on H_2-He and the final values actually used are shown in Table II.

TABLE II. Interaction potential parameters for H_2-H_2 in a.u. (1 a.u. distance $=0.529\times10^{-8}$ cm; 1 a.u. energy $=27.21$ eV).

	V_{000}[a]	V_{202}	V_{224}
A[b]	3.7264	0.1315	0
c[b]	1.4706	1.6	
d[b]	0.0224	0.0	
α_{rep}	0.91	(2.26)[c]	
	(1.0)		
β_{rep}	0.165	(1.9)[c]	
	(0.31)[c]		
C_6[b]	12.14	0.254	0.0403
α_6	0.57	1.35	
β_6	0.0	0.26	
C_8[b]	215.2	12.18	0.929
α_8	0.86	2.0	
β_8	0.20	1.5	
C_{10}[b]	4813.0	307.2	41.67
α_{10}	1.15	1.6	
β_{10}	0.40	3.8	

[a]The final interaction potential used in the calculations is V_{000}; the other terms are shown for comparison (see text).

[b]Values taken from Ref. 32.

[c]These values are taken directly from the H_2-He potential; the final optimized values are shown without parentheses.

Table II also shows the coefficient values obtained by NWB for the rigid-rotor H_2-H_2 interaction, i.e., $V_{rep}(r_0,r_0,R)$ and $C_n(r_0,r_0,R)$. Comparing these coefficients for the angle-independent V_{000} terms with those for the angle-dependent terms, one sees that the V_{000} coefficients are 15—50 times larger than the V_{202} values and 100—300 times larger than the V_{224} values.

Since the α and β values are comparable in V_{000}, V_{202}, and V_{224}, it is clear that vibrational perturbations in the H_2-H_2 collision system will be dominated by V_{000}. Calculation of γ_v and δ_v therefore requires only V_{000}, and the rest of the interaction potential can be neglected. The H_2 rotational degree of freedom is unaffected by V_{000}, and the only role rotation plays in the γ_v,δ_v calculation is to define the initial and final j values, which affect the vibrational wave functions and matrix elements parametrically.

To summarize, the interaction potential V_I used in the calculations below is given by V_{000} and depends only on the radial coordinates r_1, r_2, and R. It has the functional form given in Eq. (14) with Eqs. (15), (19), (20), and (21) substituted therein. The parameter values are given in Table II. The r_1,r_2 dependence of the long-range terms was derived from H_2-He as discussed above and the expansion coefficients were not subsequently varied. The two independent expansion coefficients for the short-range term were estimated from H_2-He, but were varied from these initial values to optimize the fit to experimental shift and broadening coefficients. The sensitivity of the calculations to parameter variations and the relationship of the results here to those obtained with simpler potential functions are discussed in Sec. VII.

IV. MATRIX ELEMENTS AND TRAJECTORY CALCULATIONS

To evaluate the phase shifts $\eta_{vj;v'j'}(b,u)$ given by Eq. (12), a set of trajectories $R(t)$ was obtained by numerically solving the Hamiltonian equations of motion in the relative center-of-mass coordinates $R(t)$, $\Theta(t)$. The spherical term $V_{000}(r_0,r_0,R)$ was used as the potential, so that the angular velocity $\dot{\Theta}$ is constant. A Runge-Kutta algorithm was employed and each trajectory was begun with R large enough so that further increase made no difference in the

result. At each velocity u trajectories were obtained for 15 impact parameters from $b=0$–9.8×10^{-8} cm. Increasing b_{max} had a negligible effect on the results for all u. Forty initial u values were chosen, representing ten collision energies equally spaced between 0.001 and 0.01 eV, ten equally spaced between 0.01 and 0.10 eV, and 20 between 0.10 and 0.50 eV. This set of b and u values was large enough to accurately perform the integrations over b and u which define the ensemble-averaged quantities γ_v and δ_v, Eqs. (10) and (11). It should be noted that the set of trajectories needs to be generated only once. The results can then be stored for use in computing γ_v and δ_v for any transition at any temperature below 500 K. Extending the calculations to higher temperature requires an extension of the u-value set to collision energies above 0.50 eV.

The only matrix elements required to evaluate Eq. (12) are $\langle v,j \mid r \mid v,j\rangle$ and $\langle v,j \mid r^2 \mid v,j\rangle$ for the v,j values corresponding to each state encountered in the set of transitions. Because the interaction potential is angle independent, only the j-dependent vibrational wave functions are required. The calculations reported here were performed with matrix elements computed from the accurate *ab initio* potential for H_2 obtained by Kolos and Wolniewicz.[2,33] Some calculations were performed with use of j-dependent Morse wave functions[34] to compute the r and r^2 matrix elements. For a given v,j state, the r-matrix elements are some 10% smaller with the Morse functions than with the exact functions; the r^2 elements differ by less than 1%. For a fixed interaction potential, the Morse function results for γ_v and δ_v are similar to those obtained with the more exact wave functions and are not further discussed.

V. EXPLICIT PHASE-SHIFT EXPRESSION

Unlike the case of foreign-gas broadening and line shifting, construction of explicit expressions for the Ψ_i and Ψ_f in the phase-shift expression Eq. (12) must take account of the effect of indistinguishability in H_2-H_2 collisions. The single-molecule transitions observed and discussed in this work are characterized by the change in v and j associated with one molecule $(0,j\rightarrow v,j')$, but the two-molecule wave functions are not, in general, simple products. For a system in which one molecule makes a transition $0,j_a\rightarrow v,j_a'$ while the collision partner remains in state $0,j_b$, the final-state symmetric $(+)$ and antisymmetric $(-)$ wave functions are

$$\Psi_f^{\pm}(\mathbf{r}_1,\mathbf{r}_2) = \frac{1}{\sqrt{2}}[\phi_{v,j_a'}(r_1)R_{j_a'}(\theta_1\phi_1)\phi_{0,j_b}(r_2)R_{j_b}(\theta_2\phi_2) \pm\phi_{0,j_b}(r_1)R_{j_b}(\theta_1\phi_1)\phi_{v,j_a'}(r_2)R_{j_a'}(\theta_2\phi_2)] . \quad (22)$$

The initial-state wave functions $\Psi_i^{\pm}(\mathbf{r}_1,\mathbf{r}_2)$ are given by the right-hand side of Eq. (22) with $v=0$ and j_a' replaced by j_a, except for the case $j_a=j_b$, for which

$$\Psi_i^{\pm}(\mathbf{r}_1,\mathbf{r}_2)=\phi_{0,j_a}(r_1)R_{j_a}(\theta_1\phi_1)\phi_{0,j_a}(r_2)R_{j_a}(\theta_2\phi_2) . \quad (23)$$

In Eqs. (22) and (23), $\phi_{v,j}$ and R_j are the normalized single-molecule wave functions for radial and angular motion. The time-integrated interaction potential can be written

$$\int_{-\infty}^{+\infty} V_I(r_1,r_2,t)dt = E(r_1+r_2) +Fr_1r_2+G(r_1^2+r_2^2) . \quad (24)$$

Substituting Eqs. (22), (23), and (24) into the phase-shift expression, Eq. (12), one obtains

$$\eta_v^{\pm} = E(\langle vj_a' \mid r \mid vj_a'\rangle-\langle 0j_a \mid r \mid 0j_a\rangle) +F[(\langle vj_a' \mid r \mid vj_a'\rangle-\langle 0j_a \mid r \mid 0j_a\rangle)\langle 0j_b \mid r \mid 0j_b\rangle] +G(\langle vj_a' \mid r^2 \mid vj_a'\rangle-\langle 0j_a \mid r^2 \mid 0j_a\rangle) \pm F\langle vj_b \mid r \mid vj_a'\rangle^2\delta(j_a',j_b) . \quad (25)$$

The symmetry-indicating superscript over η_v refers to the upper state and is independent of lower-state symmetry. The last term in Eq. (25) is zero except when the transition terminates on a j value identical to that of the nonabsorbing collision partner. This term results from symmetrization of the wave functions; when it is absent the $+$ and $-$ phase shifts are identical and equal to that calculated using a simple product form for the two-molecule wave functions.

When the last term in Eq. (25) is nonzero, there are two different phase shifts for a given, single-molecule transition, each displaced from the mean value by equal and opposite amounts. Two situations then arise. In the absence of a $+,-$ symmetry-selection rule, the net line-center shift obtained by averaging Eq. (25) over b and u is the same as that obtained without the last term. In the presence of a selection rule, e.g., only "$+$" upper states allowed, the line shift will differ from that calculated without the last term. This additional contribution to the line shift, termed the "coupling shift," has been observed in the fundamental Q-branch Raman spectrum of H_2 by May *et al.*,[13] and has been interpreted and discussed in subsequent papers.[14,17]

The coupling-shift effect is different in the electric-quadrupole spectrum than in the isotropic Raman or electric-field-induced spectra. In the latter two spectra, scattering or absorption in the two-molecule system depends on the net polarizability derivative with respect to the displacement coordinate. For isotropic Raman scattering or field-induced Q-branch absorption, the collision partners can be considered to be polarizable breathing spheres, so that only the in-phase, symmetric $(+)$ vibrational upper state is allowed, independent of the relative orientations of the collision partners. For allowed quadrupole absorption the transition moment depends on the orientation of the collision partners and there is no rigorous $+,-$ selection rule, so that the observed line-center shift is insensitive to the coupling term.

Because the coupling term is present only when the *final* j-state of the transition is the same as the (constant) j-state of the collision partner, the coupling-term magnitude differs for different transitions in an H_2 sample at equilibrium. May *et al.*[14] have expressed the line-shift coefficient for the fundamental Raman Q branch as

$$\delta=\delta_i+(n_j/n)\delta_c , \quad (26)$$

where δ_i is independent of rotational quantum number and δ_c is essentially equivalent to the contribution of the last term in the phase-shift expression, Eq. (25). The ratio n_j/n is the equilibrium fraction of molecules in state j. For H_2 at 300 K, about 65% of the molecules are in $j=1$. This means that $Q(1)$ has a larger ensemble-averaged coupling-term contribution to δ than $Q(0)$, $Q(2)$, etc. This coupling term will be small for all S-branch transitions because $j=2$ is the smallest final-state value possible, but the $O(3)$ value will be comparable to the $Q(1)$ value. Additionally, the coupling terms will be very small for all overtone transitions, because $\langle vj \mid r \mid 0j \rangle^2$ decreases rapidly as v increases.

In summary, the coupling term should have little effect on the observed line-center density shifts for any transition in the electric-quadrupole spectrum, but the coupling term produces an observable effect in certain transitions in the fundamental isotropic Raman and in the electric-field-induced Q-branch spectra.

VI. DATA ANALYSIS

The electric-quadrupole spectra of H_2 for various transitions in the 1-0 through 4-0 vibrational bands have been obtained by one of us.[9] Many of the results have been reported in previous publications,[7,8,35] although the density-broadening coefficients given here differ by 5–20% from the earlier reported values[35] because of an improved reanalysis of the collision-narrowing contribution to the linewidths.

The experimental procedures and data reduction have been described[7–9] and will be summarized only briefly here. The H_2 spectra were obtained using a Fourier-transform spectrometer (FTS) and multipass absorption cell at the National Solar Observatory of the National Optical Astronomy Observatories, Tucson, Arizona. The resolution was 0.009 cm^{-1}, permitting full resolution of all spectral features. The multipass absorption cell has a base path length of 6 m, and the actual path length was 483 m. All measurements were made at room temperature ($\sim$296 K) and the H_2 pressure ranged from 80 kPa (0.8 atm) to 270 kPa (2.7 atm). This high-pressure limit was dictated by the mechanical characteristics of the multipass cell. Because these quadrupole-absorption features are weak, particularly the overtones, most of the results discussed were obtained at the highest pressure.

Molecular hydrogen and diatomic hydrides are unusual in that their cross sections for pressure-broadening collisions are appreciably smaller than the gas-kinetic cross section, about 2 orders of magnitude smaller for self-broadening in H_2. For H_2 the small broadening cross sections allow ready observation of collision narrowing. As first discussed by Dicke,[36] velocity-changing collisions in an absorber in the absence of broadening lead to a linewidth that is smaller than the Doppler width. The extent of this narrowing depends on the collision frequency, and the resulting linewidth is more or less inversely proportional to the perturber density. Collision broadening is directly proportional to the perturber density in the binary collision approximation, so the net result is a linewidth which first decreases and then increases with increasing

TABLE III. Effective diffusion coefficients for S-branch transitions.

Line	$\bar{D}$ ($cm^2 s^{-1}$ at 25 °C and 1 amagat)
1-0 $S(1)$	1.30
2-0 $S(1)$	1.27
3-0 $S(1)$	1.23
4-0 $S(1)$	1.18

TABLE IV. Experimental and calculated electric-quadrupole line-shape parameters (in units of 10^{-3} cm^{-1} amagat^{-1} at 296 K).

	Experiment[a]		Calculation[b]	
Line	δ	γ	δ_v	γ
1-0 $Q(1)$	−2.13(4)	2.4(4)	−1.9	
$Q(2)$	−2.0(1)	2.8(3)	−1.9	
$Q(3)$	−2.2(2)	3(1)	−1.9	
$Q(4)$	−2(2)		−1.9	
$S(0)$	−1.8(1)	2.8(3)	−2.1	2.2
$S(1)$	−1.9(1)	2.6(7)	−2.2	2.6
$S(2)$	−1.4(1)	3.1(9)	−2.3	2.2
$S(3)$	−2.0(2)	2.3(5)	−2.4	2.3
2-0 $Q(1)$	−4.8(2)	4.6(7)	−3.8	4.9
$Q(2)$	−4(3)	5.5(7)	−3.8	5.3
$Q(3)$	−4(4)	5.5(7)	−3.8	5.5
$S(0)$	−4.5(9)	4.7(6)	−4.0	4.9
$S(1)$	−4.3(3)	4.8(6)	−4.1	5.3
$S(2)$	−4(3)	4.5(6)	−4.2	5.0
$O(2)$	−5(5)	3(1)	−3.6	4.4
$O(3)$	−5(10)	3(1)	−3.5	4.6
3-0 $Q(1)$			−5.8	9.7
$Q(2)$			−5.8	10.3
$Q(3)$			−5.8	10.5
$S(0)$		7.5(9)	−6.0	9.8
$S(1)$		8.5(9)	−6.1	10.4
$S(2)$		11(1)	−6.2	10.3
$S(3)$		9(1)	−6.3	10.7
4-0 $Q(1)$			−7.8	17.6
$Q(2)$			−7.8	18.1
$Q(3)$			−7.8	18.5
$S(0)$		10(1)	−8.0	17.9
$S(1)$	−8.0(5)	11(1)	−8.1	18.6
$S(2)$		10(1)	−8.2	18.7
$S(3)$		14(1)	−8.3	19.3

[a]Parentheses indicate uncertainty in the last significant figure.

[b]The calculated γ is given by the sum $\gamma_R+\gamma_v$. The values of γ_R for S- and O-branch transitions are given in Table I. An approximate γ_R for the Q branch is obtained by subtracting the calculated γ_v from the experimental γ value for each 1-0 $Q(J)$; the results are used to obtain γ values for the 2-0 through 4-0 Q branches.

TABLE V. Comparison of various experimental line-shape parameters at 300 K (in units of 10^{-3} cm^{-1} $amagat^{-1}$).

	Electric quadrupole data							
	This work		Other values		Raman data		Field-induced data	
Line	δ	γ	δ	γ	δ	γ	δ	γ
1-0 $S(0)$	−1.8(1)	2.8(3)	−1.67[a]					
$S(1)$	−1.9(1)	2.6(7)	−2.40[a]	1.64[a,b]				
$S(2)$	−1.4(1)	3.1(9)	−3.53[a]					
$S(3)$	−2.0(2)	2.3(5)	−1.77[a]					
1-0 $Q(1)$	−2.13(4)	2.4(4)	−2.40[a]		−4.5[e]	1.0[e]	−3.6[l]	1.1[l]
					−3.1[f]	0.7[j]		0.9[m]
					−3.2[g]	0.9[k]		
					−3.0[h]	0.8[h]		
					−3.1[i]			
$Q(2)$	−2.0(1)	2.8(4)			−3.4[e]	1.3[h]	−2.6[l]	1.8[l]
					−2.1[f]	1.3[j]		1.6[m]
					−2.2[i]			
$Q(3)$	−2.2(2)	3(1)			−3.3[e]	2.8[h]	−1.4[l]	2.8[l]
					−2.3[f]	1.9[j]		2.3[m]
					−2.0[i]			
2-0 $S(1)$	−4.3(3)	4.8(6)	−4.5[c]					
4-0 $S(1)$	−8.0(5)	11(1)	−8.6[d]					

[a]Reference 4.
[b]Reference 10.
[c]Reference 5.
[d]Reference 6.
[e]Reference 13.
[f]Reference 14.
[g]Reference 15.
[h]Reference 16.
[i]Reference 17.
[j]Reference 18.
[k]Reference 19.
[l]Reference 11.
[m]Reference 12.

density. In the quadrupole H_2 spectra discussed here, the minimum linewidth in the 2-0 overtone band occurs at about 2.5 amagat and is about 60% of the zero-density Doppler width.

In order to extract density-broadening coefficients from the quadrupole data, the Galatry profile[37] was used to fit the various lines. This function was derived from a soft-collision model for collision narrowing, i.e., small velocity changes per collision, and includes collision broadening as a statistically independent process. The Galatry line is characterized by specifying the Doppler width and then obtaining the diffusion coefficient D and collision-broadening coefficients γ which give the best statistical fit to the data.

The Galatry profile is not the only line-shape function which has been employed to include collision narrowing. A hard-collision model developed by Nelkin and Ghatak[38] has been used for H_2 as well. Murray and Javan[16] have compared both models to their fundamental-band Raman data, and conclude that neither model is perfect, although the hard-collision model is somewhat better when a large density range is considered. The Galatry profile was used here because a computationally convenient algorithm is available,[39] and because the best fit to both the Galatry and Nelkin and Ghatak line shapes leads to essentially the same γ and D values.[16] Furthermore, the Galatry profile provides a better fit in the density region corresponding to the minimum linewidth,[16] which is the region in which the quadrupole spectra were obtained.

It proved difficult to obtain unambiguous γ and D values from the numerical fitting algorithm when both parameters were allowed to vary simultaneously. At a given density, more than one pair of γ and D values lead to a statistically equivalent Galatry fit. In other words, such a pair of Galatry line shapes differ by less than the random noise in the data. These rms noise levels range from about 3% of the maximum absorption in 4-0 $S(1)$ to 0.1% in 1-0 $S(1)$. To eliminate ambiguity in the fits, the value of D was fixed for each transition and the γ value was varied to obtain the best fit. Were it not for the maximum-pressure limitation in the multipass cell, the γ values could have been determined unambiguously by increasing the H_2 density to a few tens of amagats. This option was not available, so the reported γ values are based on four densities from 0.8 to 2.6 amagat in the 1-0 Q branch, two densities (1.4 and 2.6 amagat) in the 1-0 S branch and 2-0 overtones, and one density (2.6 amagat) for the 3-0 and 4-0 overtones.

Choosing the proper D value for these various transitions requires some consideration. For the fundamental band, the value of H_2 self-diffusion at 25 °C ($D = 1.34$ $cm^2 s^{-1}$ $amagat^{-1}$) is usually chosen.[16,19] This experimental value[40] for diffusion of para hydrogen into normal hydrogen corresponds to all molecules in $v = 0$. When a sequence of overtone transitions is considered, one must account for the significant increase in the average H_2 internuclear separation with v. This increase implies a higher gas kinetic collision frequency and smaller D value than that appropriate to the vibrational ground state. Moreover, the requirement of identical emission and absorption

line shapes implies that neither the upper- nor the lower-state D value is correct, but an average of the two should be used. We define a state-dependent D value based on a simple rigid-sphere model[41] as

$$D_{vj}=1.34\left[\frac{2\langle 01\mid r\mid 01\rangle}{\langle vj\mid r\mid vj\rangle+\langle 01\mid r\mid 01\rangle}\right]^2 \text{ cm}^2\,\text{s}^{-1}\,\text{amagat}^{-1} \tag{27}$$

and the resulting average value for absorption from the ground state as

$$\overline{D}_{vj}\cong\tfrac{1}{2}(1.34+D_{vj})\text{ cm}^2\,\text{s}^{-1}\,\text{amagat}^{-1} \tag{28}$$

at 25 °C.

Table III lists $\overline{D}_{vj}$ for a sequence of $S(1)$ transitions. The experimental broadening coefficients γ were obtained using the appropriate $\overline{D}_{vj}$ and are shown in Table IV. These γ (HWHM) values must be considered less accurate than the experimental line-shift coefficients δ, also shown in Table IV, because they are more sensitive to the line-shape function.

The experimental line-shape parameter values obtained for the electric-quadrupole transitions are compared with literature values in Table V; most of the earlier data are for Raman Q-branch transitions in the fundamental band. Note that the quadrupole δ values for the fundamental band will not contain a coupling-shift contribution and thus should be somewhat smaller than the values for Raman and field-induced measurements. Note also that the Raman and field-induced 1-0 Q-branch γ values are appreciably smaller than the corresponding quadrupole values. Both Raman scattering and field-induced absorption in the Q branch are dominated by isotropic (tensor order $k=0$) processes whereas quadrupole absorption is an anisotropic ($k=2$) process. Energetically elastic reorientation collisions make a contribution to the rotational component of γ for $k=2$ processes, but not for $k=0$ processes.[26,28] The quadrupole Q- and S-branch γ values are therefore expected to be of comparable magnitude, and both should be larger than the Raman or field-induced Q-branch values. The data in Table V verify these relationships.

VII. DISCUSSION OF THE CALCULATION AND COMPARISON WITH DATA

As stated in Sec. II, the interaction potential was arbitrary to the extent that α_{rep} and β_{rep} values were varied to optimize the overall data fit. We originally assumed that these two parameters could be varied independently to optimize the δ_v and γ_v values for 4-0 $S(1)$, and then taken as fixed for the rest of the transitions. As Fig. 1 shows, this is not the case. The calculated δ_v values are very sensitive to β_{rep} for a given α_{rep} value; choosing α_{rep} essentially fixes β_{rep} for reasonable agreement with experiment. In addition, for any pair of α_{rep},β_{rep} values which give agreement with the experimental line shift, the calculated broadening coefficient is essentially the same.

Given the definitions, Eqs. (17) and (18), β_{rep} should be positive, so that α_{rep} must be less than 1.05. If the repulsive interaction is approximately exponential in r, then $\beta_{\text{rep}}\approx\frac{1}{2}\alpha_{\text{rep}}^2$. As Fig. 1 shows, decreasing α_{rep} requires an increase in β_{rep} to maintain agreement between the experimental and calculated δ values. For α_{rep} less than 0.75, the required β_{rep} value corresponds to an interaction which increases much more rapidly than exponentially. Within the limits $1.05\geqq\alpha_{\text{rep}}\geqq 0.75$, the calculated δ_v values increase linearly with upper-state vibrational quantum number in both the S and Q branches, but the slopes of the δ_v-versus-v curves vary. For agreement with the experimental 1-0 $S(1)$ shift as well as the 4-0 $S(1)$ shift, a value of $\alpha_{\text{rep}}=0.9$ (± 0.05) is required. The actual values used to obtain the calculated results shown in Table IV are listed in Table II. One obvious conclusion from the foregoing discussion is that the line-shift coefficients place much more stringent requirements on the choice of potential parameters than do the broadening coefficients. An interaction potential chosen to reproduce broadening coefficients alone will not necessarily be adequate for calculating line shifts. In Tables IV and VI we have assumed that the total δ value is essentially equal to δ_v. The contribution of the pure rotational line shift is known to be small in H_2.[42]

The calculated S-branch broadening coefficients reported in Table IV were obtained by adding experimental γ_R values obtained from the pure rotational S branch to the γ_v values calculated here [cf. Eq. (8) and the subsequent discussion]. The same set of γ_R values was used for the two O-branch lines since γ_v is the same for $S(J)$ and $O(J+2)$, and γ_R does not depend on the direction of the

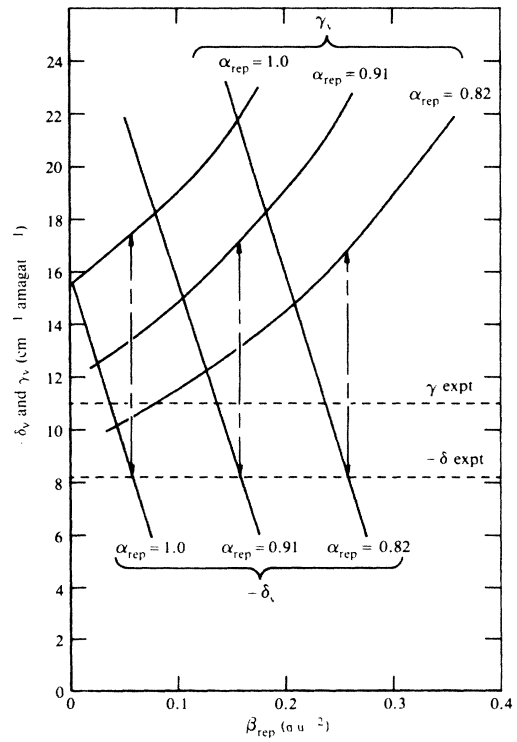

FIG. 1. β_{rep} dependence of δ_v and γ_v for fixed values of α_{rep}. The dashed vertical lines connect the calculated γ_v values which correspond to δ_v values in agreement with experiment for a given value of α_{rep}.

TABLE VI. Comparison of experimental and calculated electric-quadrupole Q-branch line-shift coefficients and experimental Raman results with coupling shift removed[a] (in units of 10^{-3} cm^{-1} amagat^{-1}).

Line	Temperature (K)	Quadrupole δ Expt.	Calc.	Raman δ_i[a]
1-0 $Q(1)$	500		4.3	
4-0 $Q(1)$	500		21	
1-0 $Q(1)$	400		1.3	
4-0 $Q(1)$	400		6.0	
1-0 $Q(1)$	296	−2.13(4)	−1.9	−1.5(1)
1-0 $Q(2)$	296	−2.0(1)	−1.9	−1.5(1)
1-0 $Q(3)$	296	−2.2(2)	−1.9	−1.5(1)
4-0 $Q(1)$	296		−7.8	
1-0 $Q(1)$	224		−4.0	−4.1(1)
4-0 $Q(1)$	224		−18	
1-0 $Q(1)$	160		−6.0	−6.0(1)
4-0 $Q(1)$	160		−17	
1-0 $Q(1)$	85		−8.5	−8.6(3)
4-0 $Q(1)$	85		−39	

[a]From the data in Ref. 17; see Eq. 26.

j-changing transition. The 2-0 Q-branch values were obtained by subtracting γ_v from the 1-0 Q-branch experimental γ values to obtain γ_R. These γ_R values were then used in conjunction with the calculated γ_v for the 2-0 Q branch.

The calculated line shifts are in good agreement with the quadrupole data for the 1-0 through 4-0 S-branch transitions and the 1-0 and 2-0 Q-branch results. The calculated pressure-broadening coefficients also agree well with the data except for the 4-0 overtone, for which the calculation overestimates the data by ~50–80%. It is apparent from Table IV that both the line-shift coefficient data and calculation lead to a nearly linear dependence on vibrational quantum number. This result had been anticipated,[43] and a linear dependence has been explicitly calculated for H_2-He systems.[44] The broadening-coefficient calculation results in a quadratic v dependence for γ_v, such that γ_v is ~33% of the total γ for the fundamental but is 90% of the total for the 4-0 overtone.

The linear δ and quadratic γ vibrational dependences are an inevitable consequence of the physical model used to describe these collision phenomena. That is, for any interaction potential in which the r dependence is expanded through quadratic terms, the sequence of $0,j \rightarrow v,j'$ phase shifts η_v for each value of u and b depend linearly on v. This results from the nearly linear v dependence of $[\langle vj' \mid r \mid vj' \rangle - \langle 0j \mid r \mid 0j \rangle]$ and $[\langle vj' \mid r^2 \mid vj' \rangle - \langle 0j \mid r^2 \mid 0j \rangle]$.

We have verified by direct calculation that the ensemble-averages $\overline{\sin\eta_v}$ and $(1-\overline{\cos\eta_v})$ can be accurately replaced by $\overline{\eta_v}$ and $\frac{1}{2}\overline{\eta_v^2}$ for $v \leq 4$; consequently δ_v is linear and γ_v is quadratic in v.

A consequence of the calculated quadratic γ_v dependence is the impossibility of significantly improving the agreement between the experimental and calculated 4-0 S-branch broadening coefficients without worsening the agreement for the 1-0 through 3-0 transitions. There is no set of interaction potential parameters within the context of the physical model that can lead to agreement for all four upper v levels. Nonetheless, the agreement between the set of calculated and experimental quadrupole shift and broadening coefficients taken as a whole is satisfactory.

Although the quadrupole absorption data were taken at 296±1 K, there are some Raman measurements for the fundamental band at lower temperatures. In order to further compare the calculations to experiment, the temperature dependences of the calculated δ_v and γ_v were obtained and are shown in Table VI (δ_v) and Fig. 2 (γ_v) for a few transitions. The calculated temperature dependence of the 1-0 $Q(1)$ quadrupole shift below 300 K is in good agreement with the experimental Raman values of Looi *et al.*[17] for the shift *without* the coupling term [δ_i in Eq. (26)]. There seems to be no available data for the temperature dependence of γ. The curves in Fig. 2 reflect only the vibrational contribution γ_v; however, for the 4-0

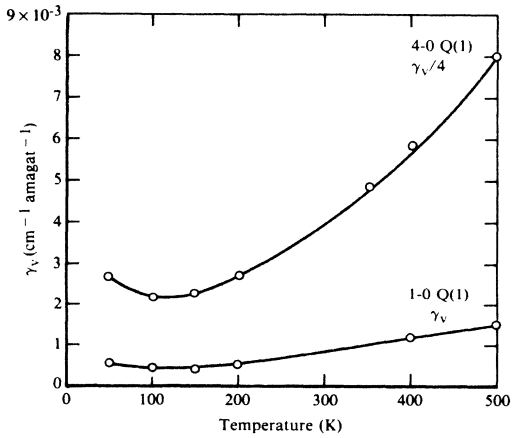

FIG. 2. Calculated temperature dependence for the vibrational contribution to the line-broadening coefficient in the 1-0 and 4-0 $Q(1)$ transitions.

overtone the vibrational effect dominates and $\gamma \simeq \gamma_v$.

The origin of the temperature dependence in δ_v can be seen in Fig. 3, which shows the contributions of each term in the interaction potential [Eq. (14)] to the net phase shift integrated over impact parameter as a function of collision energy. As the collision energy decreases below 0.02 eV, the contribution of the attractive terms, particularly the $1/R^6$ term, increases relative to that of the repulsive term. It is apparent that the thermal-average phase shift asymptotically approaches a constant positive value, i.e., a blue line-center shift, as the temperature increases toward 1000 K or so.

Several other conclusions can be drawn from Fig. 3. The phase-shift contributions from all of the attractive terms in the interaction potential are significant, and each is appreciably larger in magnitude than the net phase shift for collision energies above 0.02 eV. The small net line shift observed at room temperature is coincidental in a sense, resulting from the near cancellation of positive and negative phase shifts in the thermal average. The much larger line shifts observed with He (Ref. 13) (blue shift) or Ar (Ref. 13) (red shift) as collision partners for H_2 are easily understandable. Helium is less polarizable and Ar more polarizable than H_2, and relatively small changes in the attractive interaction will result in large changes in the net phase shift.

As Fig. 3 shows, the contribution of each potential term increases rapidly for collision energies below 0.01 eV. In this low-energy regime the effect of the attractive H_2-H_2 well, about 0.004 eV deep,[29] becomes important. For collision energies below 0.005 eV there exists a critical impact parameter $b^*(E)$ such that every collision trajectory with $b < b^*$ spirals into the repulsive wall.[45] For $b \simeq b^*$, the time required for completion of the collision increases substantially; the phase shifts associated with those trajectories become large enough that the replacement of $\sin\eta$ by η in Eq. (11) is not a good approximation, particularly for the 4-0 overtone. The subset of trajectories for which $\sin\eta \neq \eta$ is not large enough to significantly affect the thermal average in H_2-H_2, but this observation is not necessarily valid for other systems with stronger net interactions.

The low-collision-energy (<0.01 eV) regime with its large net phase shifts is particularly important in accurately calculating δ_v. At 300 K, this energy regime accounts for approximately 50% of the total thermally averaged δ_v. The broadening coefficient is much less sensitive to low-energy collisions, with only 10% of the total γ_v at 300 K resulting from collisions with energies less than 0.01 eV.

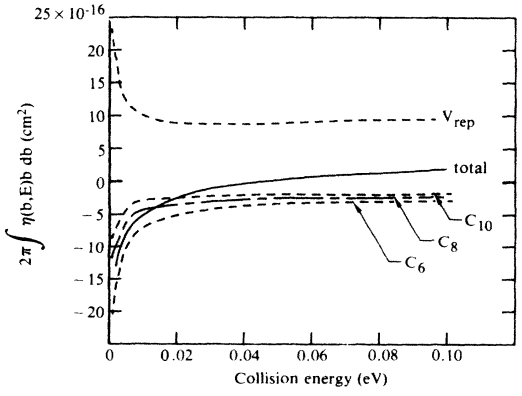

FIG. 3. Individual contributions of each term in the interaction potential to the phase-shift cross section as functions of collision energy.

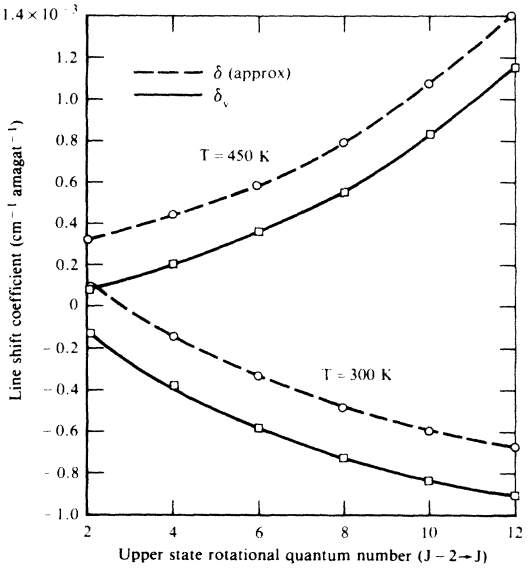

FIG. 4. Rotational state dependence of the line-shift coefficient for pure rotational transitions.

Although vibrational transitions are emphasized in this work, it is worth noting that the coupling between rotation and vibration leads to a vibrational contribution to the line shift and broadening coefficients even in the pure rotational S-branch spectrum. The calculated vibrational contribution to the broadening coefficient γ_v for 0-0 $S(0)$ through 0-0 $S(10)$ is less than 1×10^{-4} cm^{-1} amagat^{-1} and is therefore small compared to the rotational contribution γ_R (see Table I). The calculated vibrational contribution to the line-shift coefficient δ_v is displayed in Fig. 4 for two temperatures. The absolute values increase roughly by an order of magnitude from 0-0 $S(0)$ to 0-0 $S(10)$. Cooper, May, and Gupta[42] have measured δ (i.e., $\delta_v+\delta_R$) for 0-0 $S(0)$ and 0-0 $S(1)$ to be approximately 1×10^{-4} cm^{-1} amagat^{-1}. Taking this δ value for $S(0)$ and combining it with the calculated δ_v, one estimates $\delta_R \approx 2.5\times10^{-4}$ cm^{-1} amagat^{-1}. This value is about 10% of the line-shift coefficient for the fundamental vibrational band and makes a decreasing relative contribution for the overtone sequence.

The approximate total line-shift curves, shown in Fig. 4, were generated by taking this estimated δ_R value and adding it to the calculated δ_v's. The main point to be drawn from Fig. 4 is that, for high-j rotational transitions in pure H_2, the line shift is not correctly calculated by a rigid-rotor approximation. The line-shift coefficients in the H_2 rotational spectrum with He (blue shift) or Ar (red shift) as a perturber are observed[42] to be about ten times larger than that for pure H_2. This is almost certainly a vibrational effect, with δ_v accounting for most of the shift, just as in the vibrational spectrum. One can anticipate on

this basis that the observed rotational transition line shifts in H_2-He and H_2-Ar mixtures will increase in magnitude with upper state j values.

As mentioned previously, the coupling-shift coefficient term δ_c in Eq. (26) does not contribute to the line shift in the quadrupole spectra. The effect of δ_c in the Raman and field-induced Q-branch fundamentals is clear and important, however. An optimum choice of the interaction potential should permit calculation of the coupling-shift contribution to the total Raman line shift with an accuracy comparable with the results already described. The interaction potential used here does not lead to agreement with the observed[14,17] coupling term; the calculated coupling shift is an order of magnitude too small. No variation of α_{rep} and β_{rep} in the interaction potential reproduced the observed value [$\sim 1.1\times 10^{-3}$ $\text{cm}^{-1}\,\text{amagat}^{-1}$ for 1-0 $Q(1)$] and simultaneously preserved agreement with the extensive quadrupole data set. May *et al.*[14] and Looi *et al.*[17] encountered the same difficulty in obtaining agreement using a calculation based on a Lennard-Jones model for the H_2-H_2 interaction potential. They concluded that only the attractive term contributed to the coupling shift, and discarded the repulsive-term contribution. Had we suppressed the repulsive term in our calculation, agreement with the experimental value could have been obtained, but there is no physical justification for this procedure. Each term in the interaction potential, taken as a Taylor series in r_1, r_2, contributes $\alpha_i^2 r_1 r_2$ to the coupling shift, where α_i is the linear r coefficient in the expansion ($\alpha_i = \alpha_{\text{rep}}$, α_6, etc.). One cannot use α_{rep} without using α_{rep}^2 as well, but this is what selectively suppressing the repulsive contribution to the coupling shift implies.

One possible solution to this problem would be incorporation of an explicit R dependence into the potential parameters α_{rep} and β_{rep}; the H_2-H_2 potential of MHK shows this characteristic. We chose not to do this because it would require two more adjustable parameters to fit a single quantity, i.e., δ_c. A better solution would be calculation of an *ab initio* H_2-H_2 interaction potential at the same level of accuracy as the H_2-He potential. The resulting function could be then optimized as necessary using the existing data set and a calculation like that presented here.

VIII. CONCLUDING REMARKS

The calculations discussed above show that the vibrational phase shift suffices to explain the observed v dependence of both line shift and broadening coefficients in vapor-phase molecular hydrogen. Furthermore, the rotational and vibrational contributions to broadening in hydrogen are separable; as one progresses to high overtones, the vibrational contribution increasingly dominates the total broadening coefficient. A distinction between isotropic Raman (or electric-field-induced) and electric-quadrupole spectra was made with regard to the coupling shift. The coupling shift was shown to be important only in the Raman or field-induced Q branch, and there only for the fundamental vibrational band. The intermolecular interaction potential used in these calculations was generated by extending the rigid-rotor potential of NWB (Ref. 29) to include an explicit H-H separation dependence. By construction, this potential fits the thermodynamic and scattering data discussed in Ref. 29 as well as the line-shape parameters.

It is important to realize that the nearly complete separation of rotational and vibrational effects on the line shapes, while valid for H_2 and D_2, will lose its validity for molecular species in which rotationally inelastic and reorientation probabilities are large. For such a molecule, e.g., CO, pressure broadening is dominated by rotational effects with little vibrational dependence. Moreover, the line shift is much less than that expected simply by averaging the phase shift over all collisions.

Note added in proof. The room-temperature Raman Q-branch broadening coefficients for 1-0 $Q(0)$ through 1-0 $Q(3)$ obtained by Toich, Melton, and Roh[46] should be added to those listed in Table V. These values are close to those obtained by Allin *et al.*[18] as shown in Table V. The recent work of Bischel and Dyer[47] should also be noted. They obtain temperature-dependent Raman line-shift and broadening coefficients for 1-0 $Q(0)$ and 1-0 $Q(1)$. Their room-temperature 1-0 $Q(0)$ broadening coefficient is about 10% smaller than the value given in Ref. 12 (see Table V), and their 1-0 $Q(1)$ value is almost identical to that in Ref. 19 (Table V). Bischel and Dyer[47] utilize the temperature-dependent line-shift data to obtain the δ_i coefficient as in Eq. (26). These δ_i values are in good agreement with the calculated δ values shown in Table VI.

ACKNOWLEDGMENTS

This work was supported by the McDonnell Douglas Independent Research and Development program. The authors are grateful to D. E. Jennings for suggesting the calculations of the vibrational line-shift contribution to the pure rotational spectrum. We also thank K. C. Smyth and G. H. Rosasco for helpful comments on this work, and in particular for discussions on the relationship between broadening coefficients for the Raman and electric quadrupole Q-branch transitions. We are grateful to W. K. Bischel for useful discussions and for acquainting us with his work in collaboration with M. J. Dyer.

[1]A. R. W. McKellar, Icarus **22**, 212 (1974).
[2]W. Kolos and L. Wolniewicz, J. Chem. Phys. **43**, 2429 (1965).
[3]G. Herzberg, Can. J. Phys. A **28**, 144 (1950).
[4]D. H. Rank, U. Fink, and T. A. Wiggins, Astrophys. J. **143**, 980 (1966).
[5]C. Chackerian, Jr. and L. P. Giver, J. Mol. Spectrosc. **58**, 339 (1975).
[6]J. T. Bergstralh, J. S. Margolis, and J. W. Brault, Astrophys. J. **224**, L39 (1978).
[7]J. W. Brault and W. H. Smith, Astrophys. J. **235**, L177 (1980).
[8]S. L. Bragg, J. W. Brault, and W. H. Smith, Astrophys. J. **263**, 999 (1982).
[9]S. L. Bragg, Ph.D. thesis, Washington University, 1981.
[10]T. C. James, J. Opt. Soc. Am. **59**, 1602 (1969).

[11]H. L. Buijs and H. P. Gush, Can. J. Phys. **49**, 2366 (1971).
[12]R. H. Hunt, W. L. Barnes, and P. J. Brannon, Phys. Rev. A **1**, 1570 (1970).
[13]A. D. May, V. Degen, J. C. Stryland, and H. L. Welsh, Can. J. Phys. **39**, 1769 (1961).
[14]A. D. May, G. Varghese, J. C. Stryland, and H. L. Welsh, Can. J. Phys. **42**, 1058 (1964).
[15]P. Lallemand, P. Simova, and G. Bret, Phys. Rev. Lett. **17**, 1239 (1966).
[16]J. H. Murray and A. Javan, J. Mol. Spectrosc. **42**, 1 (1972).
[17]E. C. Looi, J. C. Stryland, and H. L. Welsh, Can. J. Phys. **56**, 1102 (1978).
[18]E. J. Allin, A. D. May, B. P. Stoicheff, J. C. Stryland, and H. L. Welsh, Appl. Opt. **6**, 1597 (1967).
[19]A. Owyoung, Opt. Lett. **2**, 91 (1978).
[20]P. W. Anderson, Phys. Rev. **76**, 647 (1949).
[21]C. J. Tsao and B. Curnutte, J. Quant. Spectrosc. Radiat. Transfer **2**, 41 (1962).
[22]W. B. Nielsen and R. G. Gordon, J. Chem. Phys. **58**, 4131 (1973).
[23]J. Fiutak and J. Van Kranendonk, Can. J. Phys. **40**, 1085 (1962).
[24]J. Fiutak and J. Van Kranendonk, Can. J. Phys. **41**, 21 (1963).
[25]E. W. Smith, M. Giraud, and J. Cooper, J. Chem. Phys. **65**, 1256 (1976).
[26]R. G. Gordon, J. Chem. Phys. **44**, 3083 (1966).
[27]R. A. J. Keijser, J. R. Lombardi, K. D. Van den Hout, B. C. Sanctuary, and H. F. P. Knaap, Physica **76**, 585 (1974).
[28]J. Van Kranendonk, Can. J. Phys. **41**, 433 (1963).
[29]M. J. Norman, R. O. Watts, and U. Buck, J. Chem. Phys. **81**, 3500 (1984).
[30]J. Schaefer and W. Meyer, J. Chem. Phys. **70**, 344 (1979).
[31]W. Meyer, P. C. Hariharan, and W. Kutzelnigg, J. Chem. Phys. **73**, 1880 (1980).
[32]U. E. Senff and P. G. Burton, J. Phys. Chem. **89**, 797 (1985).
[33]These matrix elements were kindly supplied by C. Chackerian in a private communication.
[34]C. L. Pekeris, Phys. Rev. **45**, 98 (1934).
[35]W. D. Cochran and W. H. Smith, Astrophys. J. **271**, 859 (1983).
[36]R. H. Dicke, Phys. Rev. **89**, 472 (1953).
[37]L. Galatry, Phys. Rev. **122**, 1218 (1961).
[38]M. Nelkin and A. Ghatak, Phys. Rev. **135**, A4 (1965).
[39](a) F. Herbert, J. Quant. Spectrosc. Radiat. Transfer **14**, 943 (1974); (b) for corrections to some of the equations in (a) see P. L. Varghese and R. K. Hanson, Appl. Opt. **23**, 2376 (1984).
[40]P. Harteck and H. W. Schmidt, Z. Phys. Chem. **21B**, 447 (1933).
[41]J. O. Hirschfelder, C. F. Curtis, and R. B. Bird, *Molecular Theory of Gases and Liquids* (Wiley, New York, 1954), p. 14.
[42]V. G. Cooper, A. D. May, and B. K. Gupta, Can. J. Phys. **48**, 725 (1970).
[43]D. H. Rank, B. S. Rao, P. Sitaram, A. F. Slomba, and T. A. Wiggins, J. Opt. Soc. Am. **52**, 1004 (1962).
[44]G. E. Hahne and C. Chackerian, Jr., J. Chem. Phys. **73**, 3223 (1980).
[45]The impact parameter $b^*(E)$ is the value for which the centrifugal potential energy barrier for relative radial motion is equal to the collision energy E. At this precise b value the scattering angle and phase shift are infinite. See the discussion in Ref. 41, pp. 45–51.
[46]A. M. Toich, D. W. Melton, and W. B. Roh, Opt. Commun. **55**, 406 (1985).
[47]W. K. Bischel and M. J. Dyer, Phys. Rev. A **33**, 3113 (1986).